JACS
JOURNAL OF THE AMERICAN CHEMICAL SOCIETY

COMMUNICATION

pubs.acs.org/JACS

MoS_2 Nanoparticles Grown on Graphene: An Advanced Catalyst for the Hydrogen Evolution Reaction

Yanguang Li, Hailiang Wang, Liming Xie, Yongye Liang, Guosong Hong, and Hongjie Dai*

Department of Chemistry, Stanford University, Stanford, California 94305, United States

Supporting Information

ABSTRACT: Advanced materials for electrocatalytic and photoelectrochemical water splitting are central to the area of renewable energy. In this work, we developed a selective solvothermal synthesis of MoS_2 nanoparticles on reduced graphene oxide (RGO) sheets suspended in solution. The resulting MoS_2/RGO hybrid material possessed nanoscopic few-layer MoS_2 structures with an abundance of exposed edges stacked onto graphene, in strong contrast to large aggregated MoS_2 particles grown freely in solution without GO. The MoS_2/RGO hybrid exhibited superior electrocatalytic activity in the hydrogen evolution reaction (HER) relative to other MoS_2 catalysts. A Tafel slope of ~41 mV/decade was measured for MoS_2 catalysts in the HER for the first time; this exceeds by far the activity of previous MoS_2 catalysts and results from the abundance of catalytic edge sites on the MoS_2 nanoparticles and the excellent electrical coupling to the underlying graphene network. The ~41 mV/decade Tafel slope suggested the Volmer−Heyrovsky mechanism for the MoS_2-catalyzed HER, with electrochemical desorption of hydrogen as the rate-limiting step.

Hydrogen is being vigorously pursued as a future energy carrier in the transition from the current hydrocarbon economy.[1] In particular, sustainable hydrogen production from water splitting has attracted growing attention.[1−3] An advanced catalyst for the electrochemical hydrogen evolution reaction (HER) should reduce the overpotential and consequently increase the efficiency of this important electrochemical process.[3] The most effective HER electrocatalysts are Pt-group metals. It remains challenging to develop highly active HER catalysts based on materials that are more abundant at lower costs.[4]

MoS_2 is a material that has been commonly investigated as a catalyst for hydrodesulfurization.[5] Recent work showed MoS_2 to be a promising electrocatalyst for the HER. Both computational and experimental results confirmed that the HER activity stemmed from the sulfur edges of MoS_2 plates, while their basal planes were catalytically inert.[6−8] As a result, nanosized MoS_2 with exposed edges should be more active for HER electrocatalysis than materials in bulk forms. Previously, MoS_2 catalysts supported on Au,[7] activated carbon,[6] carbon paper,[8] or graphite[9] were prepared by physical vapor deposition or annealing of molybdate in H_2S. Various overpotentials (from ~0.1 to ~0.4 V)[10] and Tafel slopes (55−60 mV/decade[7] or > 120 mV/decade[8]) were reported. The mechanism and reaction pathways of the HER with MoS_2 catalysts also remained inconclusive.

In recent years, our group has been developing syntheses of nanostructured metal oxide or hydroxide materials on graphene sheets, using either graphene on solid substrates or graphene oxide (GO) sheets stably suspended in solution.[11−15] These metal oxide− or hydroxide−graphene hybrids are novel because of the chemical and electrical coupling effects and the utilization of the high surface area and electrical conductance of graphene, leading to advanced materials for nanoelectronics,[11] energy storage devices (including pseudocapacitors[13] and lithium ion batteries[14]), and catalysis.[15] Here we report the first synthesis of MoS_2 on reduced graphene oxide (RGO) sheets and demonstrate the high HER electrocatalytic activity of the resulting MoS_2/RGO hybrid with low overpotential and small Tafel slopes.

The MoS_2/RGO hybrid was synthesized by a one-step solvothermal reaction of $(NH_4)_2MoS_4$ and hydrazine in an *N*,*N*-dimethylformamide (DMF) solution of mildly oxidized graphene oxide (GO; see Figure S1 in the Supporting Information)[14] at 200 °C (Figure 1A; nominal C/Mo atomic ratio ~10; see the Supporting Information for synthetic details). During this process, the $(NH_4)_2MoS_4$ precursor was reduced to MoS_2 on GO and the mildly oxidized GO transformed to RGO by hydrazine reduction.[16] Figure 2A,B shows scanning electron microscopy (SEM) images of the resulting MoS_2/RGO hybrid, in which the RGO sheets were uniformly decorated with MoS_2 nanoparticles. The transmission electron microscopy (TEM) image (Figure 2C) shows that most of the MoS_2 nanoparticles lay flat on the graphene, with some possessing folded edges exhibiting parallel lines corresponding to the different layers of MoS_2 sheets (number of layers = 3−10; Figure 2C inset). High-resolution TEM revealed hexagonal atomic lattices in the MoS_2 basal planes and abundant open edges of the nanoparticles (Figure 2D).

The MoS_2/RGO hybrid was characterized by X-ray diffraction (XRD), and the broad diffraction peaks (Figure 2E) indicated nanosized MoS_2 crystal domains with hexagonal structure [powder diffraction file (PDF) no. 771716]. Raman spectroscopy revealed the characteristic peaks[17] of MoS_2 at 373 and 400 cm^{-1} and the D, G, and 2D bands of graphene in the hybrid (Figure 2F). The uniform distribution of MoS_2 on RGO was confirmed by micro-Raman imaging of the two components in the hybrid deposited on a substrate (Figure S2). X-ray photoelectron spectroscopy (XPS) confirmed the reduction of GO to RGO and Mo(VI) to Mo(IV)[18] (Figure S3). The residual oxygen content in the hybrid was measured to be <4 atom % (Figure S3).

Importantly, GO sheets provided a novel substrate for the nucleation and subsequent growth of MoS_2. The growth of MoS_2

Received: February 10, 2011
Published: April 21, 2011

ACS Publications © 2011 American Chemical Society

dx.doi.org/10.1021/ja201269b | *J. Am. Chem. Soc.* 2011, 133, 7296–7299

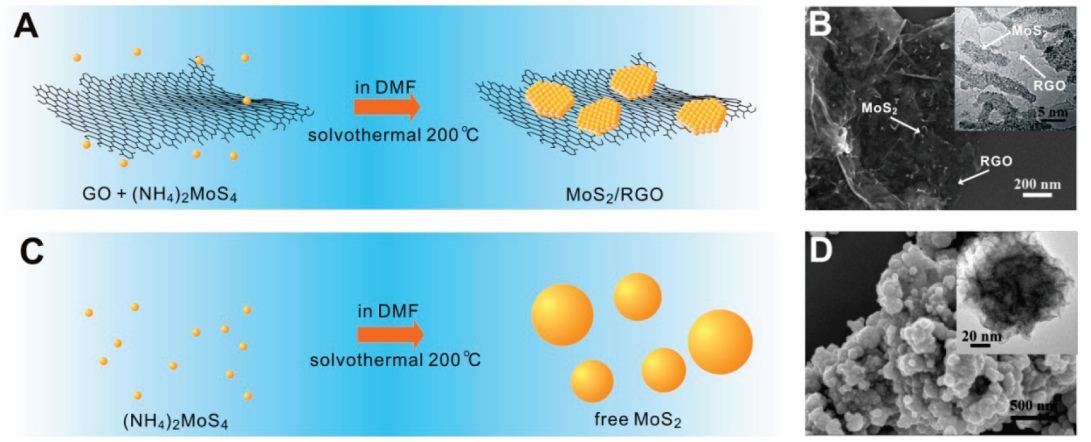

Figure 1. Synthesis of MoS_2 in solution with and without graphene sheets. (A) Schematic solvothermal synthesis with GO sheets to afford the MoS_2/RGO hybrid. (B) SEM and (inset) TEM images of the MoS_2/RGO hybrid. (C) Schematic solvothermal synthesis without any GO sheets, resulting in large, free MoS_2 particles. (D) SEM and (inset) TEM images of the free particles.

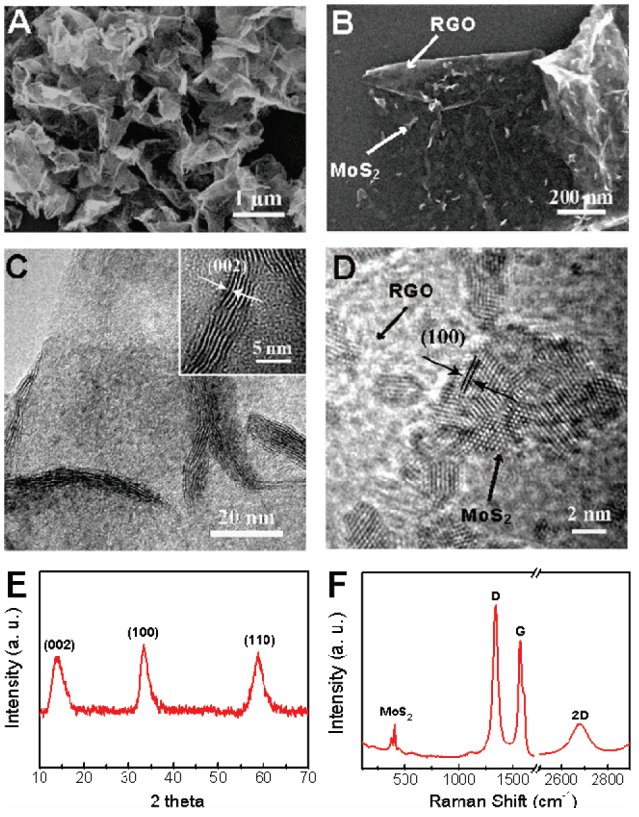

Figure 2. MoS_2 nanoparticles on graphene in the MoS_2/RGO hybrid. (A, B) SEM images of the MoS_2/RGO hybrid. (C) TEM image showing folded edges of MoS_2 particles on RGO in the hybrid. The inset shows a magnified image of the folded edge of a MoS_2 nanoparticle. (D) High-resolution TEM image showing nanosized MoS_2 with highly exposed edges stacked on a RGO sheet. (E) XRD pattern and (F) Raman spectrum of the hybrid.

was found (by microscopy and Raman imaging) to be selective on GO, with little free particle growth in solution. The selective growth on GO was attributed to the interactions between functional groups on GO sheets and Mo precursors in a suitable solvent environment.[12,14,15] In strong contrast, in the absence of GO, the exact same synthesis method produced MoS_2 coalesced into 3D-like particles of various sizes (Figure 1D). The drastic morphological difference highlights the important role of GO as a novel support material for mediating the growth of nanomaterials. It is also important to note that replacing DMF with H_2O as the solvent afforded only two separate phases of MoS_2 particles and RGO sheets (Figure S4).

We investigated the electrocatalytic HER activities of our MoS_2/RGO hybrid material deposited on a glassy carbon electrode in 0.5 M H_2SO_4 solution using a typical three-electrode setup (see the Supporting Information for experimental details). As a reference point, we also performed measurements using a commercial Pt catalyst (20 wt % Pt on Vulcan carbon black) exhibiting high HER catalytic performance (with a near zero overpotential). The polarization curve (i–V plot) recorded with our MoS_2/RGO hybrid on glassy carbon electrodes showed a small overpotential (η) of ~0.1 V for the HER (Figure 3A), beyond which the cathodic current rose rapidly under more negative potentials. In sharp contrast, free MoS_2 particles or RGO alone exhibited little HER activity (Figure 3A). MoS_2 particles physically mixed with carbon black at a similar C:Mo ratio also showed performance inferior to that of MoS_2/RGO (Figure S5). The linear portions of the Tafel plots (Figure 3B) were fit to the Tafel equation ($\eta = b \log j + a$, where j is the current density and b is the Tafel slope), yielding Tafel slopes of ~30, ~41, and ~94 mV/decade for Pt, the MoS_2/RGO hybrid, and free MoS_2 particles, respectively.

The MoS_2/RGO hybrid catalyst was further evaluated by depositing it onto carbon fiber paper at a higher loading of 1 mg/cm^2 to reach high electrocatalytic HER currents and comparing the results with literature data for MoS_2 catalysts at similar loadings (Figure 3C). At the same potential, the MoS_2/RGO hybrid catalyst afforded significantly higher (iR-corrected) HER current densities than the previous MoS_2 catalysts.[6−9]

Three possible reaction steps have been suggested for the HER in acidic media.[19] First is a primary discharge step (Volmer reaction):

$$H_3O^+ + e^- \rightarrow H_{ads} + H_2O$$

$$b = \frac{2.3RT}{\alpha F} \approx 120 \text{ mV} \qquad (1)$$

where R is the ideal gas constant, T is the absolute temperature, $\alpha \approx 0.5$ is the symmetry coefficient,[19] and F is the Faraday constant. This step is followed by either an electrochemical

dx.doi.org/10.1021/ja201269b | J. Am. Chem. Soc. 2011, 133, 7296–7299

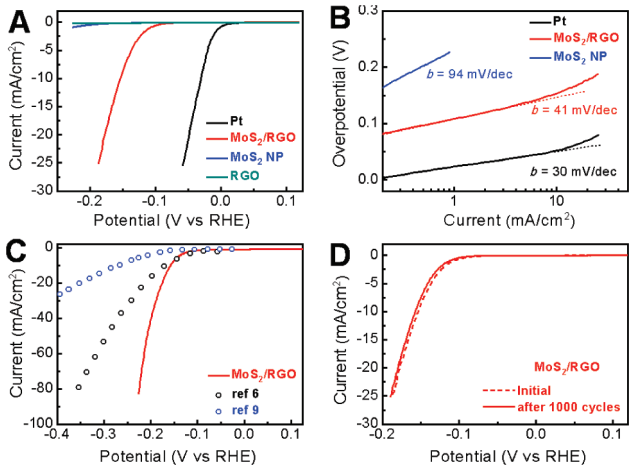

Figure 3. (A) Polarization curves obtained with several catalysts as indicated and (B) corresponding Tafel plots recorded on glassy carbon electrodes with a catalyst loading of 0.28 mg/cm^2. (C) Polarization curve recorded on carbon fiber paper with a loading of 1 mg/cm^2 (red line), in comparison with two literature results with similar catalyst loadings (blue and black ○). (D) Durability test for the MoS_2/RGO hybrid catalyst. Negligible HER current was lost after 1000 cycles from −0.3 to +0.7 V at 100 mV/s.

desorption step (Heyrovsky reaction),

$$H_{ads} + H_3O^+ + e^- \rightarrow H_2 + H_2O$$

$$b = \frac{2.3RT}{(1+\alpha)F} \approx 40 \text{ mV} \qquad (2)$$

or a recombination step (Tafel reaction),

$$H_{ads} + H_{ads} \rightarrow H_2 \qquad b = \frac{2.3RT}{2F} \approx 30 \text{ mV} \qquad (3)$$

The Tafel slope is an inherent property of the catalyst that is determined by the rate-limiting step of the HER. The determination and interpretation of the Tafel slope are important for elucidation of the elementary steps involved. Having a very high H_{ads} coverage ($\theta_H \approx 1$), the HER on a Pt surface is known to proceed through the Volmer−Tafel mechanism (eqs 1 and 3), and the recombination step is the rate-limiting step at low overpotentials, as attested by the measured Tafel slope of 30 mV/decade.[19] Unfortunately, the reaction mechanism on MoS_2 has remained inconclusive since its first HER study more than 40 years ago.[20] Even though previous density functional theory calculations suggested an H_{ads} coverage of 0.25−0.50,[6] which could favor an electrochemical desorption mechanism, experimental mechanistic studies were inconclusive because of the discrepancy of the wide range of HER Tafel slopes reported.[7,8] The observed Tafel slope of ~41 mV/decade in the current work is the smallest measured to date for a MoS_2-based catalyst, suggesting that electrochemical desorption is the rate-limiting step[19] and thus that the Volmer−Heyrovsky HER mechanism (eqs 1 and 2) is operative in the HER catalyzed by the MoS_2/RGO hybrid.

We attribute the high performance of our MoS_2/RGO hybrid catalyst in the HER to strong chemical and electronic coupling between the GO sheets and MoS_2. Chemical coupling/interactions afforded the selective growth of highly dispersed MoS_2 nanoparticles on GO free of aggregation. The small size and high dispersion of MoS_2 on GO afforded an abundance of accessible edges that could serve as active catalytic sites for the HER. Electrical coupling to the underlying graphene sheets in an interconnected conducting network afforded rapid electron transport from the less-conducting MoS_2 nanoparticles to the electrodes. To glean this effect, we performed impedance measurements at an overpotential of η = 0.12 V (Figure S6). The MoS_2/RGO hybrid exhibited much lower impedance [Faradaic impedance (Z_f), or charge-transfer impedance, of ~250 Ω[21]] than did the free MoS_2 particles ($Z_f \approx 10$ kΩ). The significantly reduced Z_f afforded markedly faster HER kinetics with the MoS_2/RGO hybrid catalyst.

Another important criterion for a good electrocatalyst is high durability. To assess this, we cycled our MoS_2/RGO hybrid catalyst continuously for 1000 cycles. At the end of cycling, the catalyst afforded similar $i-V$ curves as before, with negligible loss of the cathodic current (Figure 3D).

In conclusion, we have synthesized MoS_2 nanoparticles on RGO sheets via a facile solvothermal approach. With highly exposed edges and excellent electrical coupling to the underlying graphene sheets, the MoS_2/RGO hybrid catalyst exhibited excellent HER activity with a small overpotential of ~0.1 V, large cathodic currents, and a Tafel slope as small as 41 mV/decade. This is the smallest Tafel slope reported to date for a MoS_2 catalyst, suggesting electrochemical desorption as the rate-limiting step in the catalyzed HER. Thus, the approach of materials synthesis on graphene has led to an advanced MoS_2 electrocatalyst with highly competitive performance relative to various HER electrocatalytic materials.

■ ASSOCIATED CONTENT

Supporting Information. Experimental procedures and supporting data. This material is available free of charge via the Internet at http://pubs.acs.org.

■ AUTHOR INFORMATION

Corresponding Author
hdai@stanford.edu

■ ACKNOWLEDGMENT

This work was partially supported by ONR and NSF CHE-0639053.

■ REFERENCES

(1) Dresselhaus, M. S.; Thomas, I. L. *Nature* **2001**, *414*, 332.
(2) Bard, A. J.; Fox, M. A. *Acc. Chem. Res.* **1995**, *28*, 141.
(3) Walter, M. G.; Warren, E. L.; McKone, J. R.; Boettcher, S. W.; Mi, Q.; Santori, E. A.; Lewis, N. S. *Chem. Rev.* **2010**, *110*, 6446.
(4) Trasatti, S. *Adv. Electrochem. Sci. Eng.* **1992**, *2*, 1.
(5) Chianelli, R.; Siadati, M.; Perez de la Rosa, M.; Berhault, G.; Wilcoxon, J.; Bearden, R.; Abrams, B. *Catal. Rev.* **2006**, *48*, 1.
(6) Hinnemann, B.; Moses, P. G.; Bonde, J.; Jorgensen, K. P.; Nielsen, J. H.; Horch, S.; Chorkendorff, I.; Nørskov, J. K. *J. Am. Chem. Soc.* **2005**, *127*, 5308.
(7) Jaramillo, T. F.; Jorgensen, K. P.; Bonde, J.; Nielsen, J. H.; Horch, S.; Chorkendorff, I. *Science* **2007**, *317*, 100.
(8) Bonde, J.; Moses, P. G.; Jaramillo, T. F.; Nørskov, J. K.; Chorkendorff, I. *Faraday Discuss.* **2008**, *140*, 219.
(9) Jaramillo, T. F.; Bonde, J.; Zhang, J.; Ooi, B.-L.; Andersson, K.; Ulstrup, J.; Chorkendorff, I. *J. Phys. Chem. C* **2008**, *112*, 17492.

(10) Chen, Z.; Kibsgaard, J.; Jaramillo, T. F. *Proc. SPIE* **2010**, *7770*, 77700K.
(11) Wang, X.; Tabakman, S. M.; Dai, H. *J. Am. Chem. Soc.* **2008**, *130*, 8152.
(12) Wang, H.; Robinson, J. T.; Diankov, G.; Dai, H. *J. Am. Chem. Soc.* **2010**, *132*, 3270.
(13) Wang, H.; Casalongue, H. S.; Liang, Y. Y.; Dai, H. J. *J. Am. Chem. Soc.* **2010**, *132*, 7472.
(14) Wang, H.; Cui, L.-F.; Yang, Y.; Casalongue, H. S.; Robinson, J. T.; Liang, Y.; Cui, Y.; Dai, H. *J. Am. Chem. Soc.* **2010**, *132*, 13978.
(15) Liang, Y. Y.; Wang, H. L.; Casalongue, H. S.; Chen, Z.; Dai, H. J. *Nano Res.* **2010**, *3*, 701.
(16) Wang, H.; Robinson, J. T.; Li, X.; Dai, H. *J. Am. Chem. Soc.* **2009**, *131*, 9910.
(17) Chen, J. M.; Wang, C. S. *Solid State Commun.* **1974**, *14*, 857.
(18) Nielsen, J. H.; Bech, L.; Nielsen, K.; Tison, Y.; Jorgensen, K. P.; Bonde, J. L.; Horch, S.; Jaramillo, T. F.; Chorkendorff, I. *Surf. Sci.* **2009**, *603*, 1182.
(19) Conway, B. E.; Tilak, B. V. *Electrochim. Acta* **2002**, *47*, 3571.
(20) Tributsch, H.; Bennett, J. C. *J. Electroanal. Chem.* **1977**, *81*, 97.
(21) Harrington, D. A.; Conway, B. E. *Electrochim. Acta* **1987**, *32*, 1703.